PROCEEDINGS OF SCIENCE

Status and perspectives for FCC-ee Detector background studies

Andrea Ciarma,[a,*] **Manuela Boscolo,**[a] **Francesco Fransesini,**[a] **Pantaleo Raimondi,**[b] **Andrey Abramov,**[c] **Kevin Andrè**[c] **and Michael Hofer**[c]

[a] *INFN-LNF, Via E. Fermi 40, 00044 Frascati, Rome, Italy*
[b] *CERN, Switzerland*
[c] *SLAC, USA*

E-mail: andrea.ciarma@lnf.infn.it

The Future Circular Collider electron-positron (FCC-ee) is a proposed high-energy lepton collider that aims to reach unprecedented precision in the measurements of fundamental particles. Several beam related processes produce particles in the Machine-Detector Interface (MDI) region, which can adversely affect the measurements' accuracy. This work presents the beam-induced backgrounds studies at FCC-ee. The turnkey software Key4hep is used to estimate the occupancy levels induced by beam-beam interactions, beam losses due to failure scenarios, and the Synchrotron Radiation (SR) in the CLIC-Like Detector (CLD). Dedicated software are used to produce the primary particles for each of these processes: GuineaPig++ for the beam-beam interactions, X-Suite for the beam losses coming from particle transport, and BDSIM for the SR photons.

*** *FIXME: Name of conference,* ***
*** *FIXME: day-day Month YEAR* ***
*** *FIXME: Location, City, Country* ***

*Speaker

PoS(EPS-HEP2023)614

1. Introduction

FCC-ee [1] will run at unprecedented luminosity, so detectors must endure the intense particle flux generated by the beams during both collision and transport along the lattice. It is essential to understand and quantify these backgrounds in order to design suitable shielding and develop innovative solutions to minimize their impact on detector performance.

This manuscript presents the status of the machine induced background studies at FCC-ee. In Section 2 we describe the modeling of the elements in the Machine-Detector Interface (MDI) area used for simulations. In Section 3 we introduce the machine induced background sources and show the status of the occupancy studies relevant to these processes. In Section 4 we introduce a proposal for a non-local solenoid compensation scheme which would allow to remove the anti-solenoids from the MDI area, and in Section 5 we give some concluding remarks.

2. Modeling of the MDI area

A complete modeling of the elements and materials present in the Machine-Detector Interface region is required to correctly assess the background particles which arrive to the detector, including the production of secondary showers and backscattered particles. For the studies presented in this work, the detectors and MDI elements are modeled in the Key4hep framework [2], which is the tool used for particle tracking.

The engineered CAD model of the AlBeMet162 beam pipe developed by INFN-LNF, as described in [3], has been integrated into the Key4hep environment. This integration represents a significant advancement over the Conceptual Design Report [1] (CDR) model and brings several notable upgrades to the setup.

The new model features a double-layered central section designed for paraffin cooling, Copper manifolds in the elliptical chamber region, and the beam pipe separation region new model now complies with that used for impedance studies. Figure 1 provides a detailed view of the central chamber and copper cooling manifolds, along with a comparison between the new and old models of the beam pipe separation region, as they are implemented in the Key4hep setup for simulations. A significant difference respect to CDR are the dimensions of the central chamber, which now has a reduced inner radius of $R = 10\,mm$ and length $L = 180mm$ (compared to the previous dimensions of $R = 15\,mm$ and $L = 250\,mm$).

Figure 2 shows the other MDI elements present in the Key4hep model. The Final Focusing Quadrupoles (FFQs) are represented by a simple model composed of equivalent material, and their magnetic field is defined according to the latest optics in MAD-X [4]. A detailed description of the FCC-ee LumiCal [1] is incorporated. Cryostats for the antisolenoids have been integrated into the model as 2 cm thick hollow cylinders. To account for fringe effects, the magnetic field generated by the antisolenoids (namely the counter solenoid and compensating solenoid) has been imported into the model via a field map, as shown in Figure 3.

3. Backgrounds at FCC-ee

The particles produced by several unwanted processes in the MDI region are tracked using the Key4hep framework to assess the background levels. This study focused on the background

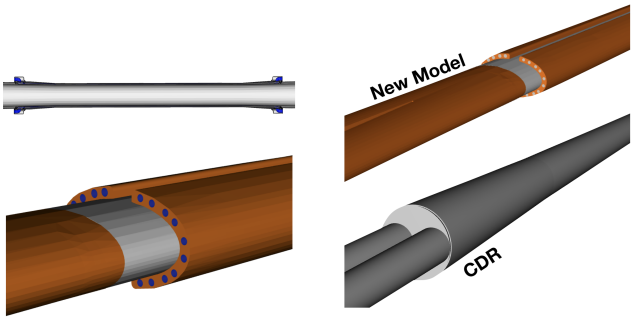

Figure 1: Left: details of the double layered central chamber with inlets and outlets for paraffine, and the Copper cooling manifolds, with the channels for water circulation. Right: comparison between the new and old Key4hep models of the beam pipe.

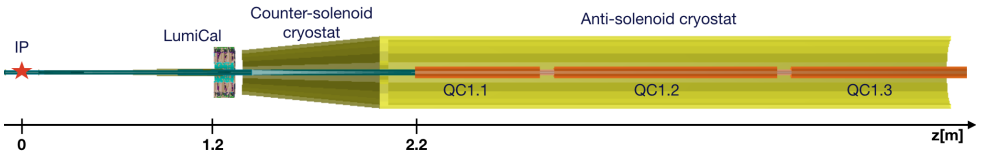

Figure 2: Elements present in the MDI region model used for simulations.

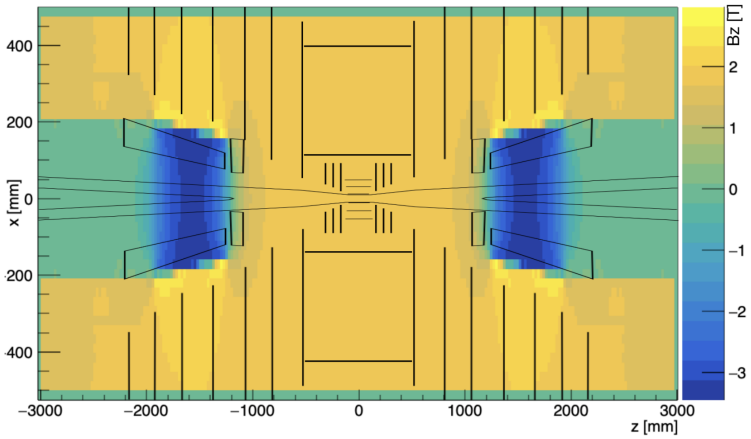

Figure 3: Magnetic field map of the 2T detector solenoid and the antisolenoids. For geometrical reference, the outline of the beam pipe and the innermost subdetectors of CLD are overlapped to the map.

induced in the CLD detector [5], in particular in the Vertex Detector (VXD) and the Inner and Outer Trackers (IT/OT, or as a single subsystem TRK). Both the VXD and TRK are Silicon based detectors, and are composed by a Barrel (B) and an Endcap (E).

The figure of merit for the background levels in the detector is the occupancy. In a silicon detector, the occupancy is the number of channels that have signal above threshold. To account for this, a cut on the energy deposited in the detectors has been set to 4 keV and 8 keV for the VXD and the TRK respectively. We assume a background to be negligible if the induced occupancy is below the 1%.

Sources of background in the MDI area can be divided in luminosity backgrounds and single-beam induced backgrounds. In the first category at FCC-ee the most relevant are the Incoherent

Pairs Creation (IPC), which consists in secondary e^-e^+ pairs produced via the interaction of the beamstrahlung photons with real or virtual photons during bunch crossing, and particles from the beam which exit the dynamic aperture after losing energy during bunch crossing due to Radiative Bhabha process. Among the single-beam induced background sources we find Synchrotron Radiation (SR) coming from the last upstream magnets, and high rates of beam losses in the IR coming from the beam halo after lifetime drop, which we refer to as *failure scenarios*. Preliminary studies exist for beam-gas (elastic, inelastic) [6] and Compton scattering on thermal photons. However, these studies need to be replicated with the new simulation framework and beam parameters and will not be discussed in this manuscript.

3.1 Incoherent Pair Creation

This process has been simulated using the generator GuineaPig++ [7] and is a well understood background in the CLD detector [8, 9]. Table 1 provides information on the maximum occupancy per detector subsystem at the four FCC-ee working points resulting from IPC. The number of produced e^+e^- pairs increases proportionally with the beam energy, as expected from the cross section. The maximum occupancy recorded for each subdetector is also larger at higher energies, but in particular for the vertex detector barrel (VXDB) it grows more rapidly with respect to the total number of pairs. This can be attributed to a larger fraction of the particles being produced within the VXD acceptance at higher energies, as highlighted by the red area in Figure 4.

The occupancy remains well below 1% at all working points in all subdetectors. However, it could become a concern when considering readout time, especially at the Z-pole due to the high repetition rate, as shown in the last two lines of Table 1.

	Z	WW	ZH	Top
Pairs produced per Bunch Crossing	1300	1800	2700	3300
Max occupancy VXD Barrel	70×10^{-6}	280×10^{-6}	410×10^{-6}	1150×10^{-6}
Max occupancy VXD Endcap	23×10^{-6}	95×10^{-6}	140×10^{-6}	220×10^{-6}
Max occupancy TRK Barrel	9×10^{-6}	20×10^{-6}	38×10^{-6}	40×10^{-6}
Max occupancy TRK Endcap	110×10^{-6}	150×10^{-6}	230×10^{-6}	290×10^{-6}
Bunch Spacing [ns]	30	345	1225	7598
Max occ. VXD w/ 1 μs pileup	2.33×10^{-3}	0.81×10^{-3}	410×10^{-6}	1150×10^{-6}
Max occ. VXD w/ 10 μs pileup	23.3×10^{-3}	8.12×10^{-3}	3.34×10^{-3}	1.51×10^{-3}

Table 1: Pairs produced per bunch crossing at the four FCC-ee working points and maximum occupancy in the VXD and TRK subdetectors of CLD, also considering the pileup effect in two arbitrary readout time windows of 1μs and 10μs.

3.2 Radiative Bhabha

During bunch crossings, beam particles can lose energy via photon emission and exit the lattice acceptance at the first quadrupoles. Particles produced using BBBrem [10] and GuineaPig++ are tracked through the beam pipe to analyze power deposition on the downstream superconductive final focus quadrupoles QC1 and QC2. These values are critical for the design of the cryostat and shieldings. Although preliminary studies suggest high power deposition on the magnets, ongoing efforts are focused on refining the simulations and the model.

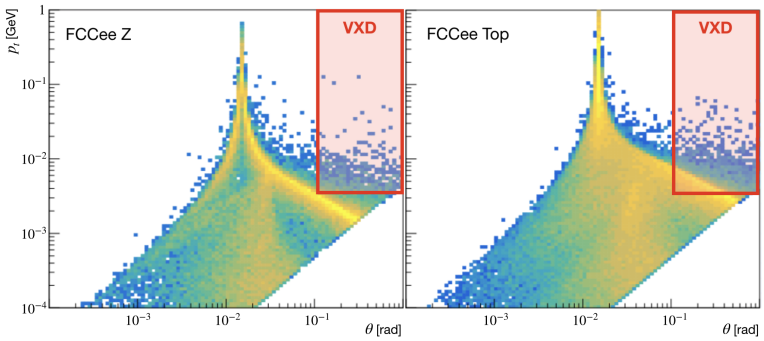

Figure 4: Production kinematics of the IPC particles emitted at FCC-ee for the Z and Top working points. The red area represents the acceptance of the CLD vertex detector (VXD).

3.3 Beam Losses due to Failure Scenarios

Several processes can increase the population of the beam halo, resulting in particle losses upon collimator impact and a reduction in beam lifetime. This situation is categorized as a failure scenario. Some of the halo particles escape the primary collimators and are propagated in the accelerator. A fraction of these particles collides with the beam pipe in the Machine-Detector Interface (MDI) region.

This study considers a scenario where the beam lifetime decreases to 5 minutes due to halo losses either on the transverse primary collimator or the off-momentum collimator. Halo particles scattered by the primary collimator are tracked for 700 turns in the FCC-ee lattice using X-Track [11].

Losses are located few meters upstream IP at all working points, in proximity of the final focus quadrupoles, both from horizontal and off-momentum collimators. Figure 5 shows the loss map around the IP due to failure scenario at the Z working point.

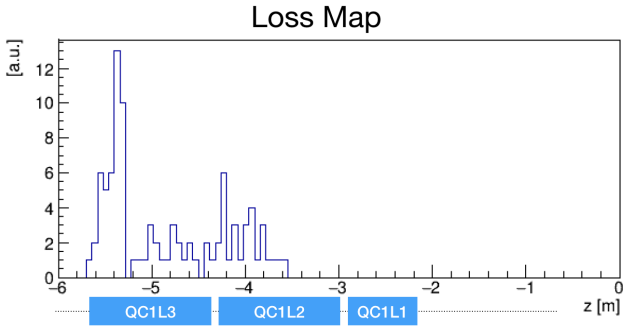

Figure 5: Beam losses upstream the IP due to failure scenario. The positions of the final focus quadrupoles are showed for reference.

Table 2 shows the maximum occupancy induced by failure scenarios in the CLD vertex detector and tracker, at the different IPs. The differences in occupancy observed at the four IPs for a given energy are primarily due to their positions relative to the location of the primary collimators at point F (PF). At the $t\bar{t}$-threshold, high occupancies of a few percent are observed, while at the Z-pole this contribution is negligible. Ongoing optimization studies are focused on mitigating this effect through adjustments to the collimators.

	Max Occupancy		Tot Power in QC1 [W]		Max Power density [W/cm^3]	
	Z-pole	$t\bar{t}$-threshold	Z-pole	$t\bar{t}$-threshold	Z-pole	$t\bar{t}$-threshold
IPA	0.02%	5.37%	0.72	1.77	0.011	0.035
IPD	<0.01%	3.99%	0.32	1.34	0.004	0.026
IPG	<0.01%	3.16%	0.18	1.09	0.003	0.013
IPJ	0.11%	8.88%	1.15	1.92	0.016	0.025

Table 2: Maximum occupancy in the CLD vertex and tracker detectors, total power and maximum power density on QC1 induced by failure scenarios on the horizontal primary collimator for the different IPs.

These particles hit the beam pipe in correspondence with the superconductive quadrupoles of the final focus, necessitating an estimation of the power deposition on these elements. Table 2 shows small values for these contributions due to beam particles being deflected by the horizontal primary collimator. Preliminary analysis on off-momentum collimators suggests the possibility of high power.

3.4 Synchrotron Radiation

Synchrotron Radiation primary photons have been generated using BDSim [12]. SR coming from the beam core is efficiently shielded by a tungsten mask located 2.13 m upstream the IP. The induced background from a round halo with dimensions from 10σ to 60σ (approximatively 90% of the aperture) is below the occupancy safety limits O(1%) as long as the tail population is under 0.001% of the total. The contribution to occupancy resulting from SR photons that are not fully absorbed by the tungsten mask and that are diffused at large angles has been found to be approximately one order of magnitude smaller than that from the halo.

4. Non-local Solenoid Compensation Scheme

The 2T detector solenoids induce coupling in the FCC-ee lattice. In the baseline lattice this is corrected using the compensating and screening solenoids, as described in Section 2. A compensation scheme similar to that used in DAΦNE [13] would allow for the removal of those solenoids, resulting in benefits such as increased available space in the MDI area. The scheme uses tilted Final Focus quadrupoles to follow the beam rotation, and skew quadrupoles correctors to control coupling correction and matching. The sign of the detectors' field at the four IPs is alternated to improve the cancelation of residual coupling. Two anti-solenoids must be introduced in order to cancel the field integral, located far from the IR and thus being on-axis respect to the beam.

A first study on this scheme performance has been performed using MAD-X [4] at the Z working point, supposing on-axis detector solenoidal fields (the realistic simulation using the 15 mrad crossing angle is ongoing). The nominal emittances at the FCC-ee Z-pole are $\epsilon_x = 0.5\,nm\,rad$ and $\epsilon_y = 1\,pm\,rad$. The coupling induced by the 2T detector solenoids at the four IPs will increase the vertical emittance up to $48\,pm\,rad$. By alternating the sign of the solenoids at the four IPs, as shown in figure 6 (left) reduces this contribution of a factor 4.

Through fine tuning of the innermost final focus quadrupoles tilt and of the skew quadrupoles, the contribution to vertical emittance has been succesfully corrected to $\epsilon_y^{coupling} = 0.018\,pm\,rad$,

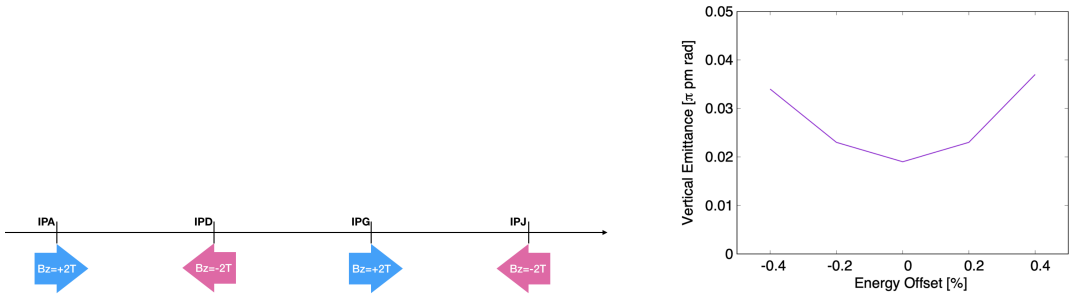

Figure 6: Left: Sketch of the 2T solenoidal field sign rearrangement at the four IPs. Right: chromatic coupling.

negligible compared to the nominal value. Figure 6 (right) shows that also the chromatic contribution to coupling is corrected.

5. Conclusions

The Key4hep modelization of the MDI region and upgrades since the CDR have been presented. A realistic model of the IR beam pipe with cooling sections is now imported from CAD designs. The magnetic field of anti-solenoids and final focus quadrupoles are implemented to provide more realistic charged particle tracking in simulations.

Luminosity backgrounds (IPC) are well understood and remain within safety limits in CLD. Failure scenarios induced backgrounds suggest potential high occupancy in tracker endcaps, but collimator optimization studies are ongoing to mitigate this effect. The power deposited in the SC final focus quadrupoles due to failure scenarios shows minimal risk of instantaneous quenching.

Estimates regarding the induced background from SR suggest that current tungsten shieldings may be removed or reduced.

More detailed studies on the power induced by Radiative Bhabha particles on the SC FFQs are required and are being performed.

A non-local solenoid compensation scheme has been proposed, potentially eliminating the need for IR anti-solenoids and freeing up space in the crowded MDI region. Initial studies demonstrate the effectiveness of this scheme in reducing the contribution to vertical emittance to a small fraction of the nominal one, even when considering chromatic effects.

Funding

This work was partially supported by the European Union's Horizon 2020 research and innovation programme under grant No 951754 – FCCIS Project.

References

[1] A. Abada *et al.* [FCC Collaboration], FCC-ee: The Lepton Collider : Future Circular Collider Conceptual Design Report Volume 2. Eur. Phys. J. ST **228** (2019) no.2, 261. https://fcc.web.cern.ch/

[2] G. Ganis *et al.*, Key4hep, a framework for future HEP experiments and its use in FCC. arXiv:2111.09874 [hep-ex]

[3] M. Boscolo, F. Palla, F. Bosi, et al. Mechanical model for the FCC-ee interaction region. EPJ Techn Instrum 10, 16 (2023). https://doi.org/10.1140/epjti/s40485-023-00103-7

[4] MAD-X, Methodical Accelerator Design. http://mad.web.cern.ch/mad

[5] N. Bacchetta *et al., CLD - A Detector Concept for FCC-ee. arXiv:1911.12230 [physics.ins-det]*

[6] M. Boscolo, O.Blanco-García, H. Burkhardt, F. Collamati, R. Kersevan, M. Lueckhof "Beam-gas Background Characterization in the FCC-ee IR", J. Phys. Conf. Ser., 1067, 2, 2018 10.18429/JACoW-IPAC2018-MOPMF085

[7] D. Schulte, Beam-Beam Simulations with GUINEA-PIG . CERN-PS-99-014-LP, http://cds.cern.ch/record/382453, Mar, 1999.

[8] A. Ciarma, M. Boscolo, G. Ganis, E. Perez, Machine Induced Backgrounds in the FCC-ee MDI Region and Beamstrahlung Radiation, Proceedings of eeFACT2022, p.85-90, 2023. 10.18429/JACoW-eeFACT2022-TUZAT0203

[9] M. Boscolo, A. Ciarma, Characterization of the beamstrahlung radiation at the future high-energy circular collider PRAB (accepted for publication)

[10] R. Kleiss, H. Burkhardt, BBBREM – Monte Carlo simulation of radiative Bhabha scattering in the very forward direction. CERN SL/94-03 (OP) January 1994

[11] Online Available: https://xsuite.readthedocs.io/en/latest/

[12] L. J. Nevay et al., BDSIM: An accelerator tracking code with particle–matter interactions, Comput. Phys. Commun. 252 107200 (2020)

[13] C. Milardi, M. Preger, P. Raimondi THE DAΦNE INTERACTION REGION FOR THE KLOE-2 RUN DAΦNE TECHNICAL NOTE, Note: IR-14, Frascati, March 29, 2010